Quantitative T1 and T2* assessment of VX2 tumour oxygenation in response to hyperoxia and hypercapnia: comparison with invasive measures and DCE-MRI

J. D. Winter[1,2], M. K. Akens[3], and H-L. M. Cheng[1,4]

[1]Physiology and Experimental Medicine, The Hospital for Sick Children, Toronto, Ontario, Canada, [2]Research and Development, IMRIS, Winnipeg, Manitoba, Canada, [3]Orthopaedic Surgery, Sunnybrook Health Sciences, Toronto, Ontario, Canada, [4]Medical Biophysics, University of Toronto, Toronto, Ontario, Canada

Introduction: Hypoxic tumour regions have a reduced response to radiotherapy and may require 2 - 3 times the radiation dose to achieve the same level of cell death. Strategies to increase tumour oxygenation is a major area of ongoing research, and typically involve altering the patient's fraction of inspired O_2 and/or CO_2 (FiO_2 and/or $FiCO_2$) alone or in combination with pharmacological agents[1]. Incorporation of noninvasive imaging of tumour oxygenation could enable subject-specific delivery of inspired gas concentrations to maximize treatment efficacy. Numerous studies employed T_1 and T_2* relaxation times to track tissue O_2 levels in normal tissue[2] and tumours[3]; however, simultaneous blood flow and volume changes during inspired gas modulation obscure the association between MR relaxation times and tissue partial pressure of O_2 (pO_2). This is further complicated in tumours due to the abnormal vasculature, variable baseline relaxation times and dependence on the host tissue response. Beyond relaxation time measurements, dynamic contrast enhanced (DCE) MRI has also shown promise as a predictor of tumour sensitivity to radiotherapy, based on the relationship between vascular characteristics and tumour hypoxia. The purpose of this study was to characterize T_1 and T_2* responses to 100 % O_2, and carbogen gas with three different CO_2 concentrations in a VX2 tumour model and compare the responses with quantitative DCE parameters, fibre optic measurements of pO_2 and microsphere measurements of tissue perfusion.

Methods: VX2 cell suspensions were injected into the thigh muscle of six New Zealand white rabbits to induce growth of a soft tissue carcinoma. MRI scans were performed 12 - 23 days following VX2 cell implantation to provide a range of tumour development. One day following the MR study, invasive tissue oxygenation and tissue perfusion measurements were obtained. Five gas challenges were delivered during MR imaging and invasive studies: i. air (21 % O_2, balanced N_2); ii. 100 % O_2; iii. 3 % CO_2 and 97 % O_2; iv. 6 % CO_2 and 94 % O_2; and, v. 9 % CO_2 and 91 % O_2. MR acquisitions were performed on a 1.5 T GE Signa EXCITE MRI, using a 3" receive-only surface coil positioned under the rabbit's thigh muscle for imaging the tumour. A separate transmit-receive knee coil for acquisition of the arterial input function (AIF) from the aorta. Quantitative T_1 values were generated for each gas using 3D FSPGR scans with three different flip angles (FA)[4]: TR = 6.55 ms, TE = 2.7 ms, FA = 2, 10 and 21°, FOV = 120 mm, matrix = 192 × 160, slice thickness (SL_{TH}) = 3 mm, number of slices (N_{SL}) = 10, NEX = 4. Quantitative T_2* measurements were collected for each gas with a 2D multi-echo GRE sequence: TR = 100 ms, 16 equally spaced TEs = [2.1 – 47.1] ms, FA = 30°, FOV = 120 mm, matrix = 192 × 160, SL_{TH} = 3 mm, N_{SL} = 6, and NEX= 3.

DCE-MRI data were collected using a dual-bolus approach. The AIF was collected in the knee coil using an initial prebolus (0.04 mmol/kg) Gd-DTPA (Magnevist, Berlex Canada) with a sagittal TRICKS acquisition that captured the aorta in one slice. Imaging parameters included: TE = 1.37 ms TR = 3.01 ms, FA = 20°, FOV = 180 mm, matrix = 90 x 90, N_{SL} = 10, SL_{TH} = 3 mm, NEX = 0.75, and temporal resolution = 0.554 s. After 15 – 25 minutes, quantitative T_1 values were collected in the tumour using the 3" surface coil. Full bolus (0.16 mmol/kg) DCE-MRI scans were then obtained using a 3D FSPGR scan with the following imaging parameters: TE = 2 ms, TR = 5.12 ms, FA = 15°, FOV = 120 mm, matrix = 128 × 96, SL_{TH} = 3 mm, N_{SL} = 10, NEX = 0.75 and temporal resolution = 2.925 s.

Image post-processing was performed offline in Matlab. T_1 maps were calculated using the SPGR steady state signal equation with flip angle correction[4]. T_2* maps were calculated using a monoexponential signal decay[5]. Regions-of-interest (ROI) were outlined on T_1 and T_2* maps in the: 1. tumour rim, 2. tumour core, 3. necrotic tumor region, and 4. normal muscle to generate mean T_1 and T_2* values for each region. For DCE quantification, the AIF was first extracted from an ROI in the aorta from the prebolus scan and converted to concentration using the linear relationship between ΔR_1 and contrast concentration. Tissue uptake curves were extracted from the four ROIs described above and converted to contrast agent concentration, using the measured T_1 values. The tissue contrast uptake curve was modeled using the adiabatic approximation tissue homogeneity model (AATH) model[6] to quantify the contrast extraction fraction (E), plasma flow (F_p), mean capillary transit time (T_c), and interstitial volume fraction (v_e).

Tissue pO_2 measurements were performed using the OxyLite system (Oxford Optronics, Oxford, UK), which utilizes fluorescence lifetime measurements to quantify absolute tissue pO_2. Two probes were inserted directly into one of the four regions isolated in MR imaging analysis (e.g., tumour periphery). Invasive perfusion measurements were performed using 15 um diameter neutron-activated microspheres.

Results: Figure 1 provides example DCE MRI images at peak contrast, with the corresponding T_1 and T_2* maps from two different rabbits. ΔT_1 and ΔT_2* values relative to air breathing (21 % O_2, balanced N_2) are reported in Table 2. We observed a consistent ΔT_1 decrease and ΔT_2* increase across all four gas challenges in all tissue regions. Effects of increasing carbogen gas CO_2 concentration on ΔT_1 and ΔT_2* are shown in Figure 3, where ΔT_1 values are consistently reduced, with a significant negative correlation was observed between ΔT_1 and $\Delta paCO_2$ in the core tumour region ($r = -0.54$, $p < 0.05$). The ΔT_2* values were variable and did not follow a trend. For the DCE-MRI data, the only significant relationship existed between F_p and ΔT_1 ($r = -0.58$, $p < 0.05$). Oxylite invasive measures of pO_2 revealed a substantial pO_2 increase at the transition to 100 % O_2 that was sustained for the duration of the experiment. Microsphere perfusion values show increased perfusion during 100 % O_2 with a small decrease after administration of 3 % CO_2 in core and necrotic regions.

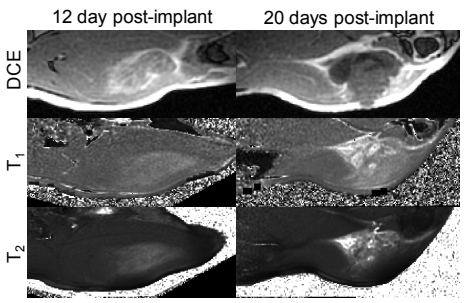

Figure 1. Example DCE image and T_1 and T_2* maps of two different tumours.

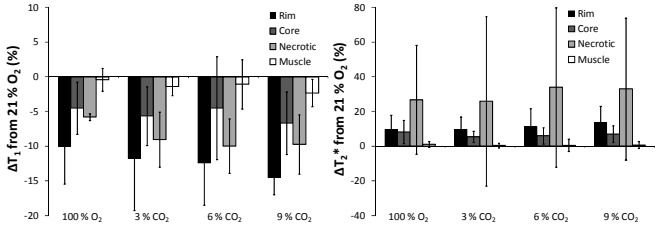

Figure 2. ΔT_1 and ΔT_2* values for each gas mixture relative to medical air (21 % O_2) for four different tissue regions.

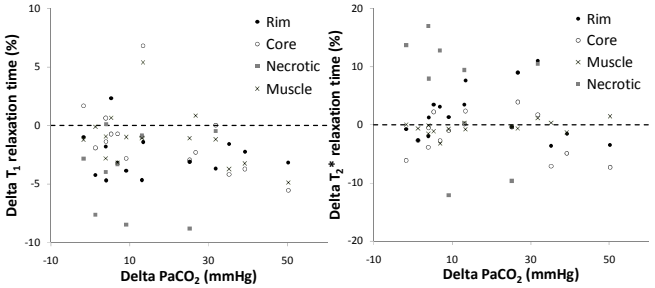

Figure 3. ΔT_1 and ΔT_2* for each carbogen gas mixture relative to 100 % O_2 versus $paCO_2$ values for four different tissue regions.

Discussion: In this study, all hyperoxic gas challenges substantially increased tumour pO_2 levels, which was reflected in decreased T_1 and increased T_2* measurements, likely due to higher dissolved oxygen and higher venous HbO_2-to-Hb ratio, respectively. A major observation was that in the VX2 tumour model, CO_2 effects in carbogen did not influence MR relaxation times compared with 100 % O_2, which suggests similar tumour oxygenation levels may be achieved with or without a CO_2 component. This observation is supported by previous work that showed independence of pO_2 levels with respect to CO_2 concentration in inhaled carbogen gas mixtures[7,8]. Results of the current study further support the use of MR relaxation times to aid adaptive strategies for improving tumour pO_2 for radiotherapy.

References: 1. Kaanders JH *et al.*, Lancet Oncol 2002, **3**:728-371; 2. O'Connor JP *et al.*, Magn Reson Med 2009, **61**:75-83; 3. Howe FA, *et al.* NMR Biomed 2001,**14**:497-506; 4. Cheng HL *et al.*, Magn Reson Med 2006, **55**:566-574; 5. Beaumont M, *et al.*, J Magn Reson Imaging 2009,**30**:313-320. 6. St Lawrence K S and Lee TY, J Cereb Blood Flow Metab 1998, **18**:1365-77; 7. Powell ME, *et al.* Radiother Oncol 1999,**50**:167-171; 8. Xia M, *et al.* Phys Med Biol 2006,**51**:45-60.